Electronic properties of 1-4, dicyanobenzene and 1-4, phenylene diisocyanide molecules contacted between Pt and Pd electrodes: First-principles study

C. Morari,[1,2,3] G.-M. Rignanese,[2,4,5] and S. Melinte[1,2]

[1]*Unité des Dispositifs Intégrés et Circuits Electroniques (DICE), Université Catholique de Louvain, 3 Place de Levant, B-1348 Louvain-la-Neuve, Belgium*

[2]*Research Center on Micro- and Nanoscopic Materials and Electronic Devices (CERMIN), Université Catholique de Louvain, B-1348 Louvain-la-Neuve, Belgium*

[3]*NIRDIMT, 71-103 Donath Str., Ro-400293 Cluj-Napoca, Romania*

[4]*Unité de Physico-Chimie et de Physique des Matériaux (PCPM), Université Catholique de Louvain, 1 Place Croix du Sud, B-1348 Louvain-la-Neuve, Belgium*

[5]*European Theoretical Spectroscopy Facility (ETSF)*

(Received 6 September 2006; revised manuscript received 19 June 2007; published 21 September 2007)

Using first-principles calculations, we study the electronic properties of 1-4, dicyanobenzene and 1-4, phenylene diisocyanide molecules sandwiched between two Pt(111) and Pd(111) electrodes. For these metal-molecule-metal systems, we calculate the total and local density of states and the charge transfers. Our results suggest that the tunneling is the dominant mechanism of charge transport. By inducing a shift of the Fermi level of about 2 eV via an additional gate electrode, the electronic transmission could be significantly increased through the metal-1-4, phenylene diisocyanide-metal systems, but a higher voltage would be required in the metal-1-4, dicyanobenzene-metal devices.

DOI: 10.1103/PhysRevB.76.115428 PACS number(s): 71.15.Mb, 73.63.Rt

I. INTRODUCTION

Molecular electronics is an emerging field of research which seeks to use individual molecules to perform functions in electronic circuitry that are now performed by traditional semiconductor devices.[1] Individual molecules are hundreds of times smaller than the features presently attained by semiconductor technology. Because it is the area taken up by each electronic element that matters, molecular electronic devices could be significantly smaller than their semiconductor-based counterparts. The dramatic reduction in size and the sheer enormity of entities offered by chemical synthesis are the main benefits of molecular electronics.

Among the different categories of potential candidates for novel molecular devices, disubstituted benzene molecules have been the subject of numerous investigations from both the theoretical[2–10] and experimental[11–14] points of view. The substitution of the end groups in the benzene structure has two distinct effects: (i) it introduces new molecular states that are end-group related and (ii) it determines the molecule-electrode interaction through the end-group bond.[2] Several recent theoretical investigations have concentrated on benzene dithiolate, which may be viewed as a benchmark system.[2–6] The interest in benzene dithiolate is partly due to the strong bond formed by sulfur with noble metal surfaces. Nevertheless, other disubstituted benzene molecules, especially coupled to technologically relevant metals for the semiconductor industry such as Pt and Pd,[13–16] are increasingly important. In a seminal conductivity study on 1-4, dicyanobenzene (DCB) connected to electrodes described by the jellium model, Lang and Avouris[7] found that the density of states (DOS) of a DCB molecule presents a sharp resonance just above the Fermi level. The corresponding orbitals do not present a significant amplitude on the anchoring groups, indicating a weak interaction between the molecule and the electrodes. As the local density of states (LDOS) on the benzene ring displays a sharp peak close to the Fermi level, the molecular device would have a high electronic transmission if the Fermi level could be shifted electrostatically with a gate electrode. Such a system is a good candidate for a molecular-field-effect transistor.[5,17] Clearly, through clever engineering of the molecular architecture, unique device characteristics could be obtained.

Many methods have been proposed to investigate the transport properties of molecular devices.[18] For all of them, the determination of the electronic structure is a key element. In particular, the relative position of the frontier (highest occupied and lowest unoccupied) molecular orbitals and the Fermi level of the metallic electrodes is of utmost importance. Among the various approaches, density-functional theory[19] (DFT) gives accurate results with an acceptable computational cost. By using DFT, we study 1-4, dicyanobenzene and 1-4, phenylene diisocyanide (PDI) molecules sandwiched between two Pt(111) and Pd(111) electrodes. Our goal is twofold: (i) to explore the particularities of the electronic structure of the DCB and PDI molecules in contact with the closest-packed surfaces of two experimental relevant materials and (ii) to bridge a gap in the fundamental understanding of the bonding of -CN and -NC groups to metal surfaces. We investigate the DOS, the LDOS, and the charge transfers (CT). We find that the coupling between the molecules and the electrodes is predominantly of physical type, indicating that tunneling is the dominant conduction mechanism.

II. TECHNICAL DETAILS

Our DFT calculations are carried out with the ABINIT package.[20] The exchange-correlation energy is evaluated within the generalized gradient approximation of Perdew,

 ©2007 The American Physical Society

Burke, and Ernzerhof.[21] Only valence electrons are explicitly considered using norm-conserving pseudopotentials to account for core-valence interactions.[22] The wave functions are expanded in plane waves with a kinetic energy cutoff of 35 hartree. For all the calculations, we use a Gaussian smearing[23] with a width of 0.01 hartree. We use a Monkhorst-Pack grid of $2\times2\times1$ k points for supercell calculations.

Our device models consist of a molecule (DCB or PDI) anchored between two metal (Pt or Pd) electrodes consisting of clusters including 26 atoms, derived from the (111) surface of the metal. We consider both top and hollow positions for the bonding of the molecule to metal surfaces, as illustrated for the case of DCB and Pt in Figs. 1(a) and 1(b), respectively. As we find that the hollow geometry is not stable (i.e., the metal-DCB-metal systems have the tendency to relax so that the N atom is always on top of a metal atom), we only consider the top configuration hereafter.

The metal-molecule-metal systems are confined into a periodic tetragonal supercell of sides $a=b=14$ Å (allowing for 10 Å vacuum between the molecules). The values of the third axis of the tetragonal cell are $c=18.69$ Å for Pt-DCB-Pt, $c=18.84$ Å for Pd-DCB-Pt, $c=18.68$ Å for Pt-PDI-Pt, and $c=18.57$ Å for Pd-PDI-Pd. These values result from the following procedure.

We first perform a structural optimization of the isolated molecule and of the bulk metals. The equilibrium lattice constants are found to be 4.04 and 3.98 Å for Pt and Pd, in good agreement with the experimental values of 3.92 and 3.89 Å, respectively. Then, we optimize the distance between the molecule and the electrode, while keeping the orientation of the N-N axis perpendicular to the surface. For the DCB molecule, we find an optimal distance of 1.91 and 2.04 Å for Pt and Pd, respectively. In the case of the PDI molecule, we obtain 1.89 and 1.90 Å for Pt and Pd, respectively. Finally, the atomic positions the metal-molecule-metal systems are relaxed until the forces are lower than 0.025 eV/Å while keeping the cell fixed. This procedure closely mimics the way in which the molecular devices are fabricated in the experiments.[24] As a result, the molecules may change their geometry due to the interaction with the metal surfaces.

The pictures representing molecular structures and the charge densities were realized using the XCRYSDEN code.[25]

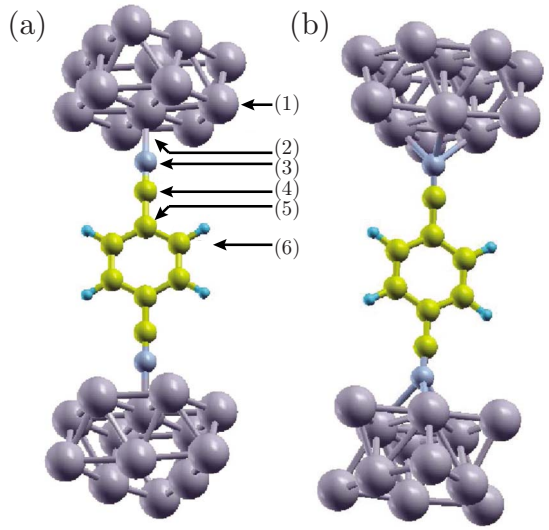

FIG. 1. (Color online) Device models used in our calculations for the Pt-DCB-Pt systems. The Pt, N, C, and H atoms are represented in gray, blue, yellow, and light blue, respectively. The DCB molecule is attached to the Pt(111) surfaces in either (a) top position or (b) hollow position. Similar models are used for the Pd(111) surfaces and for the PDI molecule (for which the positions of atoms 3 and 4 are switched).

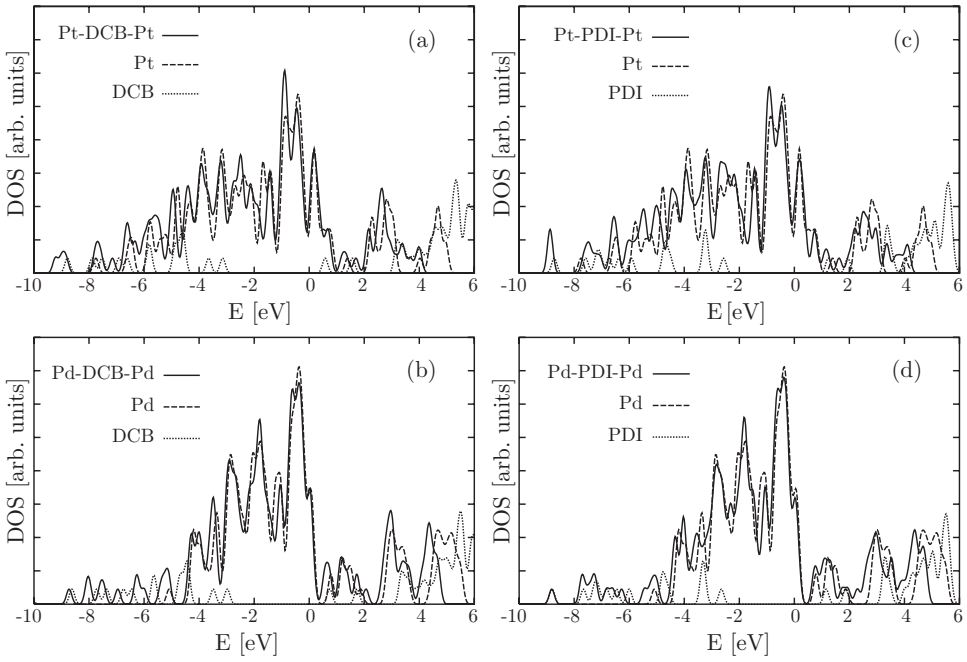

FIG. 2. DOS for (a) Pt-DCB-Pt, (b) Pd-DCB-Pd, (c) Pt-PDI-Pt, and (d) Pd-PDI-Pd (solid line). In each plot, the DOS of the corresponding isolated molecules (dotted line) and (111) metal clusters (dashed line) are also reported.

III. RESULTS

A. Density of states

We first analyze the relative position of the energy levels of the molecule with respect to the metal. In Fig. 2, the DOS of the metal-molecule-metal systems, the metal clusters, and the isolated molecules are compared for the four combinations of DCB or PDI molecules and Pt or Pd electrodes. The energies are expressed relative to the Fermi level (E_F=0) for the metal-molecule-metal systems and the metal clusters. The deepest energy levels of the molecules are aligned with the corresponding level in the metal-molecule-metal systems.

The PDI has a gap between the highest occupied molecular orbital (HOMO) and the lowest unoccupied molecular orbital (LUMO) of 3.6 eV, which is slightly smaller than the HOMO-LUMO gap of 3.9 eV obtained for DCB. The Fermi level of the electrodes lies in the HOMO-LUMO gap of the molecules, close to the LUMO level.

In order to explore the properties of the states close to the Fermi level for the four metal-molecule-metal systems, we compute their LDOS:

$$\rho(\mathbf{r},E) = \sum_i |\psi_i(\mathbf{r})|^2 \delta(E_i - E),$$

where ψ_i denote the eigenstates of the system and E_i the corresponding eigenvalues. In general, although the LDOS does not fully determine the conductivity, the regions where the LDOS is depressed are expected to be barriers for electronic transmission, while large values of the LDOS indicate a high tunneling probability. It was pointed out that the molecule-electrode coupling plays the most important role in the transport properties.[26] It is sufficient that the same orbital has significant weights at both metal contacts in order to obtain significant values for the conductivity.

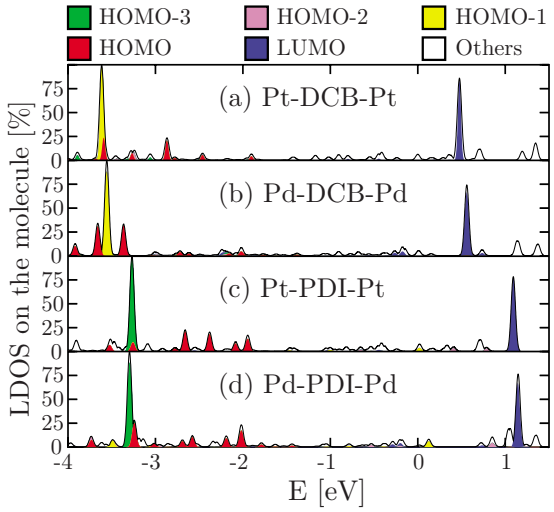

FIG. 3. (Color online) Amount of the LDOS (expressed in percent of the total LDOS) located on the molecule for the (a) Pt-DCB-Pt, (b) Pd-DCB-Pd, (c) Pt-PDI-Pt, and (d) Pd-PDI-Pd systems. The latter is decomposed into the contributions of the HOMO-3 (green), HOMO-2 (pink), HOMO-1 (yellow), HOMO (red), and LUMO (blue) orbitals of the isolated molecules (DCB or PDI). These contributions are added up one on top of the other, so that the remaining white region in the LDOS peaks has another origin (either it is the contribution of other orbitals of the isolated molecules or it does not correspond to one of these orbitals at all). The LDOS is calculated using Gaussians with a half-width of 0.06 eV to represent the δ functions.

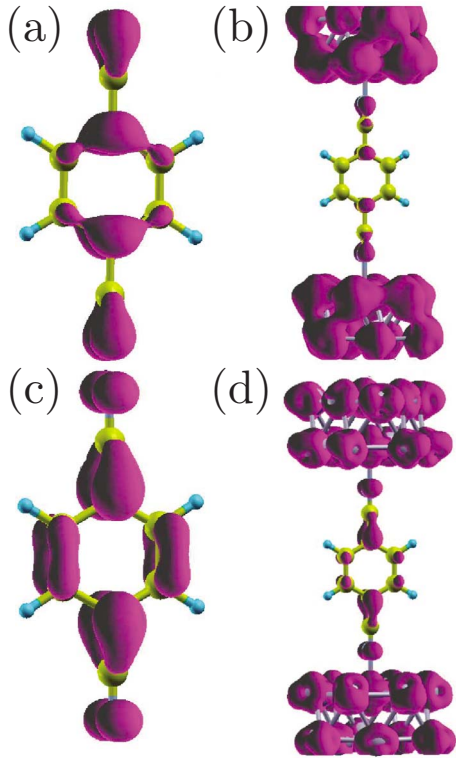

FIG. 4. (Color online) Contour plot of the HOMO and LUMO: (a) and (c) for the isolated DCB molecule and (b) and (d) for the Pt-DCB-Pt system (see text). The isosurfaces correspond to electronic densities equal to one-tenth of the maximal values (i.e., 1.4 and 1.7×10^{-3} e/Å^3 for the HOMO and the LUMO, respectively).

By artificially dividing the supercell, we separate the LDOS on the metal from that on the molecule. The amount of the LDOS located on the molecule is reported in Fig. 3. By projecting the eigenstates of the system on selected orbitals of the isolated molecules, it is possible to quantify their respective contributions to the LDOS on the molecule. The results of such projections on the HOMO-3, HOMO-2, HOMO-1, HOMO, and LUMO orbitals of the isolated molecules (DCB or PDI) are reported in Fig. 3.

In the energy range considered in Fig. 3 (from −4 to 1.5 eV), two states (one above and the other below the Fermi level) are essentially located on the molecule (75% or more of the total LDOS) for all the systems. The one above E_F originates mostly from the LUMO of the isolated molecules (blue peak located at 0.47, 0.56, 1.08, and 1.14 eV for Pt-DCD-Pt, Pd-DCB-Pd, Pt-PDI-Pt, and Pd-PDI-Pd, respectively). The one below E_F comes mostly from the HOMO-1 of the DCB molecule (yellow peak located at 3.61 and 3.56 eV for Pt-DCD-Pt and Pd-DCB-Pd, respectively) or the HOMO-3 of the PDI molecule (green peak located at 3.27 and 3.29 eV for Pt-PDI-Pt and Pd-PDI-Pd, respectively).

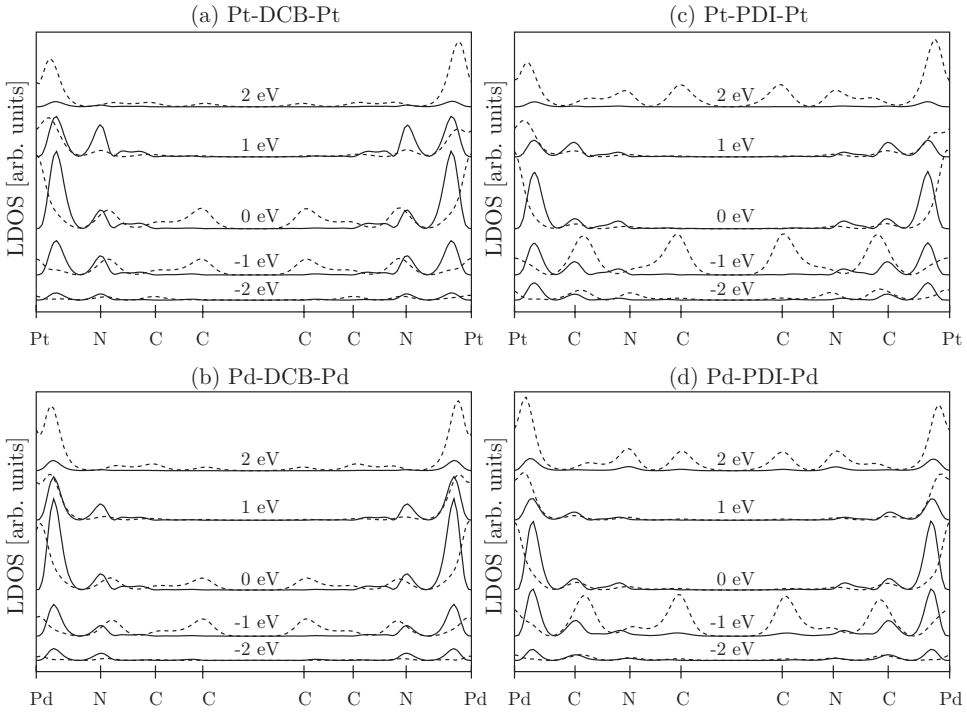

FIG. 5. LDOS at different gate bias values for (a) Pt-DCB-Pt, (b) Pd-DCB-Pd, (c) Pt-PDI-Pt, and (d) Pd-PDI-Pd systems, along the N-N axis of the system (solid line) and along the same direction but 1 Å away from the benzene plane (dotted line). For each gate bias, the LDOS is integrated between −0.5 and 0.5 eV. Positive bias values provide information about the occupied states (valence), while negative bias values convey information on the unoccupied (conduction) states.

Note that the relative position in energy of these two states of the systems is almost unchanged compared to the isolated molecules.

All the other states between −4 and 1.5 eV are essentially located on the metal. In particular, a series of peaks (indicated in red) can be associated to the HOMO of the isolated molecules. The position and the height of these peaks vary significantly from one system to another and may be responsible for the different behavior between DCB and PDI systems when a positive gate bias is applied (see discussion below). In particular, note that the peaks that appear around −2 eV in the metal-PDI-metal systems are significantly larger than in the metal-DCB-metal systems. In the Pt-PDI-Pt system, these peaks are slightly higher than those in the Pd-PDI-Pd system.

All the peaks in Fig. 3 also include contributions other than those of the HOMO, HOMO-1, HOMO-2, HOMO-3, and LUMO orbitals of the isolated molecule (the white parts). These can be the contributions of other orbitals of the isolated molecules or they may not correspond to one of these orbitals at all. Our analysis reveals that for all the peaks that we have discussed so far such contributions are in fact negligible. Indeed, they do not affect significantly the shape of the total LDOS compared to the isolated molecules. As an example, we report the LDOS integrated over an energy range of 0.07 eV around the peaks located close to −2.87 and 0.47 eV (largest red and blue peaks) for the Pt-DCB-Pt system in Figs. 4(b) and 4(d), respectively. The projections on the orbitals of the isolated molecules in Fig. 3 show that these peaks originate essentially from the HOMO (red) and LUMO (blue), for which the LDOS are also illustrated in Figs. 4(a) and 4(c), respectively. The LDOS on the molecule for the full system is similar to that of the isolated molecules. Noticeably, the coupling to the electrodes is negligible. The conclusions drawn from this example are also true for all the other peaks that we have discussed so far. As a consequence, we expect that tunneling will play an important role in the transport of electrons at small bias.

If a gate potential is applied to the device, the energy levels are shifted and the conduction mechanism may change. This effect can be analyzed through the LDOS by varying the gate bias as reported in Fig. 5. Two directions are considered for the representation of the LDOS: along the N-N axis of the system and the same direction but 1 Å away from the benzene plane. The former provides information only about the states with σ symmetry around the N-N axis, the π states being captured by the latter.

We first focus on the σ states. As expected, for all four systems, the LDOS on the benzene ring is negligible and remains essentially unchanged upon biasing the devices with a gate electrode. On the contrary, LDOS is quite important on the contact atoms for bias values ranging between −1 and 1 eV. Note that the two peaks located on the contact atoms are separated by a region in which the LDOS is close to zero. Interestingly, for higher bias values (close to ±2 eV), these σ states disappear. The LDOS on the contact atom (3) is slightly higher for the DCB devices than for the PDI ones, whereas for atom (4) it is the contrary. In all cases the N atom [(3) for DCB and (4) for PDI] displays a higher LDOS than the C atom [(3) for DCB and (4) for PDI].

When moving away from the benzene plane, π states also appear and hence the LDOS may become significant on the benzene ring. In particular, the LUMO-like peak (in blue in Fig. 3), which has a π character as illustrated in Fig. 4(c), produces an enhancement of the LDOS for a gate bias of about −0.5 and −1 eV for the DCB and PDI systems, respectively. In Fig. 5, since only integer values are considered (which is somewhat arbitrary), this contribution appears for both 0 and −1 eV gate biases for the DCB systems and only for −1 eV gate bias for the PDI systems. A further increase

of the gate bias to −2 eV results in a strongly diminished LDOS for all systems. The same is also true for a positive bias of 1 eV. In the case of the DCB systems, it remains so even for a 2 eV bias, while for the PDI systems, the LDOS on the benzene rings becomes again important. This can directly be related to the position of the principal HOMO-like peaks (in red in Fig. 3) slightly higher in energy for the PDI systems than for the DCB devices.

B. Charge transfer

We now turn to a discussion of the CT that may occur between the molecules and the electrodes. As shown in Fig. 4(c), the LUMO of the isolated molecule is divided in two parts: the first is completely delocalized on the benzene ring and the second is located on the contact atom, labeled 3 in Fig. 1 (i.e., the N atom in the case of DCB and the C atom in the case of PDI). The node between the two parts suggests that the electron transfer will take place between the contact atom and the electrode, leaving the electric charge of the benzene ring unchanged.

The CT is obtained by summing the charge densities in the metallic clusters and the isolated molecule and substracting this quantity from the charge density of the metal-molecule-metal system. The contour maps in the benzene plane[27] and in the plane passing through the N-N axis and perpendicular to the former are reported in Fig. 6.

For all systems, the CT is close to zero for the atoms of the benzene ring. At variance, the largest CT occurs between the contact atoms (i.e., atoms 2 and 3 following the notation of Fig. 1). Besides, the spatial distribution of the CT between these two atoms tends to indicate that no covalent bond is formed between the molecule and the surface.

IV. CONCLUSIONS

We have studied the electronic properties of the DCB and PDI molecules sandwiched between Pt(111) and Pd(111) electrodes using a DFT approach. We have found that the coupling between the molecules and the metal electrodes is predominantly of physical type. As a consequence, the coupling between the orbitals of the molecule and those of the metallic contacts is small. This indicates that mechanisms such as tunneling may play an important role in the conductivity at small bias, in agreement with the experimental findings. If a gate potential is applied to the system, the LDOS in the center of the benzene ring may significantly be increased. This is obtained for a negative bias of about 1 eV for both DCB and PDI systems, while for a positive bias of 2 eV, the increase of the LDOS can only be achieved in the PDI systems.

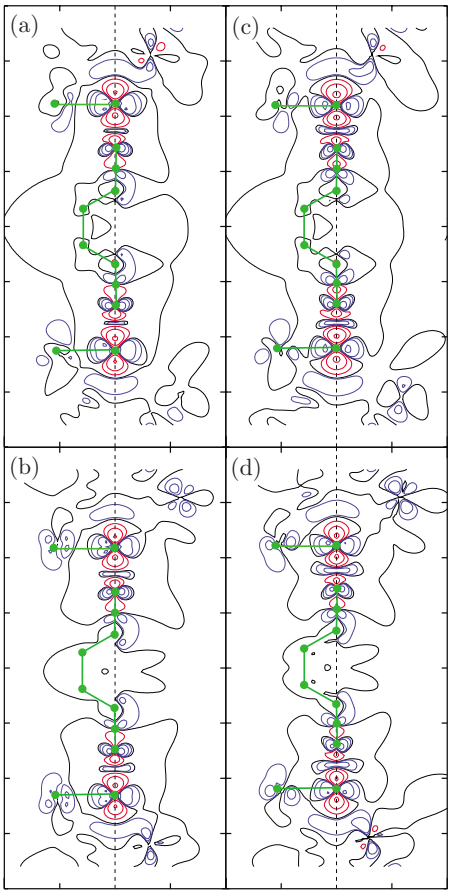

FIG. 6. (Color online) Contour plot of the charge transfer for (a) Pt-DCB-Pt, (b) Pd-DCB-Pd, (c) Pt-PDI-Pt, and (d) Pd-PDI-Pd systems. Taking advantage of the symmetry of the systems, the charge transfer is represented both in the benzene ring plane (Ref. 27) (left part) and in the plane passing through the N-N axis (dashed line) and perpendicular to the former plane (right part). The size of projection for each plane area is 10×40 Å^2. Positive, null, and negative values are represented in red, black, and blue lines. The outermost curve correspond to 75 and -11×10^{-5} $e/$Å^3. The values are multiplied by four at each successive curve.

ACKNOWLEDGMENTS

The work was supported by the Belgian FNRS and the NANOMOL project ("Actions de Recherches Concertées, Communauté Française de Belgique"). All calculations were done at CISM, Université Catholique de Louvain, in the frame of Project FRFC No. 2.4502.05 "Simulation numérique."

[1] See, for instance, edited by Marya Lieberman, *Molecules as Components of Electronic Devices*, ACS Symposium Series No. 844 (American Chemical Society, Washington, DC, 2003).

[2] Y. Xue and M. A. Ratner, Phys. Rev. B **69**, 085403 (2004).

[3] M. Di Ventra, S. T. Pantelides, and N. D. Lang, Phys. Rev. Lett. **84**, 979 (2000).

[4] S. Piccinin, A. Selloni, S. Scandolo, R. Car, and G. Scoles, J. Chem. Phys. **119**, 6729 (2003).

[5] M. Di Ventra, S. T. Pantelides, and N. D. Lang, Appl. Phys. Lett. **76**, 3448 (2000).
[6] N. Sergueev, D. Roubtsov, and H. Guo, Phys. Rev. Lett. **95**, 146803 (2005).
[7] N. D. Lang and Ph. Avouris, Phys. Rev. B **64**, 125323 (2001).
[8] W. Lu, V. Meunier, and J. Bernholc, Phys. Rev. Lett. **95**, 206805 (2005).
[9] R. Dahlke and U. Schollwöck, Phys. Rev. B **69**, 085324 (2004).
[10] Y. Choi, W. Y. Kim, K.-S. Park, P. Tarakeshwar, K. S. Kim, T.-S. Kim, and J. Y. Lee, J. Chem. Phys. **122**, 094706 (2005).
[11] M. A. Reed, C. Zhou, D. J. Muller, T. P. Burgin, and J. M. Tour, Science **278**, 252 (1997).
[12] A. Salomon, D. Cahen, S. Lindsay, J. Tomfohr, V. B. Engelkes, and C. D. Frisbie, Adv. Mater. (Weinheim, Ger.) **15**, 1881 (2003).
[13] J. Chen, L. C. Calvet, M. A. Reed, D. W. Carr, D. S. Grubish, and D. W. Bennett, Chem. Phys. Lett. **313**, 741 (1999).
[14] J. O. Lee, G. Lientsching, F. Wiertz, M. Struijk, R. A. J. Janssen, R. Egberink, D. N. Reinhoudt, P. Hadley, and C. Dekker, Nano Lett. **3**, 113 (2003).
[15] H.-G. Boyen, P. Ziemann, U. Wiedwald, V. Ivanova, D. M. Kolb, S. Sakong, A. Gross, A. Romanyuk, M. Büttner, and P. Oelhafen, Nat. Mater. **5**, 394 (2006).
[16] M. S. Islam, G. Y. Yung, T. Ha, D. R. Stewart, Y. Chen, S. Y. Yang, and R. S. Williams, Appl. Phys. A: Mater. Sci. Process. **80**, 1385 (2005).
[17] S.-H. Ke, H. U. Baranger, and W. Yang, Phys. Rev. B **71**, 113401 (2005).
[18] S. Datta, *Electronic Transport in Mesoscopic Systems* (Cambridge University Press, Cambridge, England, 1995).
[19] P. Hohenberg and W. Kohn, Phys. Rev. **136**, B864 (1964); W. Kohn and L. J. Sham, Phys. Rev. **140**, A1133 (1965).
[20] X. Gonze, J.-M. Beuken, R. Caracas, F. Detraux, M. Fuchs, G.-M. Rignanese, L. Sindic, M. Verstraete, G. Zerah, F. Jollet, M. Torrent, A. Roy, M. Mikami, Ph. Ghosez, J.-Y. Raty, and D. C. Allan, Comput. Mater. Sci. **25**, 478 (2002).
[21] J. P. Perdew, K. Burke, and M. Ernzerhof, Phys. Rev. Lett. **77**, 3865 (1996).
[22] N. Troullier and J. L. Martins, Phys. Rev. B **43**, 1993 (1991).
[23] M. Methfessel and A. T. Paxton, Phys. Rev. B **40**, 3616 (1989).
[24] In general, the fabrication of molecular devices includes two steps. First, the electrodes are created by electromigration, mechanically controllable break junctions, or other techniques. Second, the devices are completed via self-assembling procedures.
[25] A. Kokalj, J. Mol. Graphics Modell. **17**, 176 (1999). Code available from http://www.xcrysden.org/
[26] F. Remacle and R. D. Levine, Chem. Phys. Lett. **383**, 537 (2004).
[27] To be precise, the plane is defined by atoms 3 and 6 and their symmetric counterparts in the benzene ring. The other atoms in the figure (in particular those of the end groups and the metal atoms) are located at most at 0.22 Å from this plane.